A novel cuprotosis-related lncRNA signature effectively predicts prognosis in glioma patients

Xiang Yu Wang (wang_xy123@126.com)
First Affiliated Hospital of Jinan University
Augustine K. Ballah
First Affiliated Hospital of Jinan University
Wen Qian Che
First Affiliated Hospital of Jinan University
Shuaishuai Wu
First Affiliated Hospital of Jinan University

Research Article

Keywords: Cuprotosis, lncRNA, Prognosis, Prognostic Signature

Posted Date: April 18th, 2022

DOI: https://doi.org/10.21203/rs.3.rs-1549548/v1

Abstract

Cuprotosis is a novel and different cell death mechanism from the existing known ones that can be used to explore new approaches to treating cancer. Just like ferroptosis and pyroptosis, cuprotosis-related genes regulate various types of tumorigenesis, invasion and metastasis. However, the relationship between cuprotosis related long non-coding RNA (cuprotosis-related lncRNA) in glioma development and prognosis has not been investigated. We obtained relevant data from the Genotype-Tissue Expression (GTEx), Cancer Genome Atlas (TCGA), Chinese Glioma Genome Atlas (CGGA) and published articles. First, we identified 365 cuprotosis-related lncRNAs based on 10 cuprotosis-related differential genes ($|R^2|>0.4$, $p < 0.001$). Then using lasso and Cox regression analysis methods, 12 prognostic cuprotosis-related lncRNAs were obtained and constructed the CuLncSigi risk score formula. Our next step was to divide the tumor gliomas into two groups (high-risk and low-risk) based on the median risk score, and we found that patients in the high-risk group had a significantly worse prognosis. We used internal and external validation methods to simultaneously analyze and validate that the risk score model has good predictive power for patients with glioma. Next, we also performed enrichment analyses such as GSEA and aaGSEA and evaluated the relationship between immune-related drugs and tumor treatment. In conclusion, we successfully constructed a formula of cuprotosis-related lncRNAs with a powerful predictive function. More importantly, our study paves the way for exploring cuprotosis mechanisms in glioma occurrence and development, and helps to find new relevant biomarkers for glioma early identification and diagnosis and to investigate new therapeutic approaches.

Introduction

Glioma is a common and fatal primary tumor in the central nervous system. It is classified by the World Health Organization (WHO) as grade I to IV according to its histological features, and the higher the malignancy, the worse the prognosis (1). Although the current advanced surgical techniques, radiotherapy, and other comprehensive treatments bring hope to patients, their overall prognosis is still poor, getting more severe economic pressure and burden on patients themselves, their families, and society (2). Therefore, there is an urgent need for early identification and diagnosis of glioma-related biomarkers in our clinical care and novel therapeutic approaches that can improve their prognosis in the long term.

Recently, Todd Golub's team demonstrated a copper-regulated cell death-dependent mechanism distinct from known death mechanisms that occur through direct binding of copper to the lipidated components of the tricarboxylic acid (TCA) cycle, naming it cuprotosis (3). This study explains the pathology associated with hereditary copper overload disorders and suggests that cuprotosis could be a new approach to treating cancer (4). The study reported ten genes closely related to copper death. After reviewing the literature, we found previous related reports demonstrating the critical role of these genes in tumors. For example, FDX1 can closely influence the prognosis of lung adenocarcinoma through its involvement in fatty acid oxidation and amino acid metabolism (5). Dihydrothioctanamide dehydrogenase (DLD) induces ferroptosis in head and neck cancer cells by regulating cystine

deprivation(6). Upregulation of PDHA1 gene expression can inhibit the Warburg effect from inducing apoptosis in hepatocellular carcinoma(7). More importantly, with the confirmation of the specific mechanism of cuprotosis, the perfect answer to the previous question about why copper inhibits the growth of tumors was given(8). For instance, copper inhibits the activity of glioblastoma cells because cuprotosis may be involved in the development of tumor cells (9). The fact that copper complexes can affect the redox state of gliomas to act as antiproliferative may also be due to the presence of cuprotosis in gliomas(10). Therefore, cuprotosis, which reveals a novel cell death mechanism, has a great potential to become a new cancer treatment. Copper death-related genes may be critical markers for treating glioma and improving the prognosis of glioma patients. So, the construction of prognosis-related features of cuprotosis-related genes to explore their gene functions is particularly important for improving the future treatment of glioma.

Long non-coding RNA, as regulators involved in various intracellular processes, has been shown to play an essential role in epigenetics and tumorigenesis, and development. It has been shown that downregulation of lncRNA PVT1 can stop tumor growth by inhibiting glioma cell proliferation and migration (11). Knockdown of lncRNA KCNQ1OT1 enhanced tumor regression by TMZ in a mouse model of U251 glioma (12). In addition, it has also been reported that lncRNAs can be used to treat gliomas and predict their prognosis(13). Many studies have recently demonstrated that immune, iron death and pyroptosis-associated lncRNAs can be used as tumor markers. Therefore, we aimed to investigate the relevant role of cuprotosis-related lncRNAs on glioma prognosis to explore their essential mechanisms in tumor development, search for suitable new glioma biomarkers for early identification and diagnosis, and investigate other new therapeutic approaches.

Materials And Methods

Data Collection

The data used for the study included 1152 non-tumor brain tissue RNA sequence data from the GTEx database and 698 glioma RNA sequence data and clinical information from the TCGA database; the data used for validation were 1018 glioma patient RNA and clinical data from the CGGA database. All data were normalized to fragment per kilobase million (FPKM) values. When extracting clinical data, survival times less than 30 days and the presence of undocumented data collection were excluded. Cuprotosis-associated genes were obtained from those reported in the article(3). Since the data involved in this study were obtained from public databases, ethics committee approval was not required according to the relevant regulations of the databases.

Identification of Cuprotosis-related lncRNAs and Relationship with Prognosis

First, we analyzed the differential expression of genes associated with cuprotosis in glioma and normal tissues using the Wilcoxon method (FDR < 0.05, FC > 1). Subsequently, the "limma" package in R software

was used to identify lncRNAs associated with cuprotosis ($|R^2| > 0.4$, $P < 0.001$). Next, Univariate COX regression analysis was applied to calculate lncRNAs significantly related to patient prognosis. Finally, we determined the prognostic signatures of 12 cuprotosis- related lncRNAs for glioma by LASSO regression and multivariate COX regression analysis.

Construction and Validation of the Risk Score Formula

We constructed a risk score (RS) formula based on 12 prognostic signatures associated with cuprotosis.

$$\text{CuLncSigi risk score} = \sum_{i=1}^{n} \text{coef CuLncS}i\text{g}i \times \text{EXP CuLncS}i\text{g}i$$

Coef CuLncSigi and EXP CuLncSigi represent the coefficient value and the expression level of lncRNAs, respectively. TCGA patients were divided into two groups (high-risk and low-risk groups) by median risk score, and Kaplan-Meier and ROC curves were plotted. Then, we used two internal validation datasets of TCGA and an external validation dataset CGGA to validate the validity and controllability of constructing RS formulae with Prognostic cuprotosis-related lncRNAs. Finally, for the 12 cuprotosis-related lncRNAs, we compared and validated the expression levels of different grades of gliomas in TCGA samples and CGGA samples, respectively. We also constructed a nomogram and validated it.

Functional Annotation of Cuprotosis-Related lncRNAs

Functional enrichment analysis was performed using GSEA (version 4.1.0, ($P < 0.05$, $FDR < 0.25$)) (14). The infiltrating fraction of 16 immune cells and the activity of 13 immune-related pathways were measured by ssGSEA(14). We also explored the correlation of immune checkpoints between the two risk groups(15).

Prediction of Immune-related Drugs

To find more drugs for the treatment of glioma, we focused on evaluating and predicting immune-related drugs. We measured the half-maximal inhibitory concentration (IC50) of the drugs using the Wilcoxon signed-rank test.

Statistical Analysis

This study was statistically analyzed using R software (version 4.1.2) and GSEA software (version 4.1.0). Wilcoxon test was used to determine the expression levels of cuprotosis-related genes in cancer and normal tissues. Cox and Lasso's regression assessed the prognostic impact of cuprotosis-related lncRNA signatures. Survival curves were generated using the Kaplan-Meier (KM) method and compared using the log-rank test.

Results

Screening for Cuprotosis-related lncRNAs

After analyzing the TCGA database, we found that cuprotosis-related genes were significantly differentially expressed between gliomas and normal tissue (Fig. 1A). MTF1, DLD, DALAT, FDX1, LIAS, LIPT1, CDKN2A were highly expressed in tumor samples ($p < 0.001$). PDHB, PDHA1, and GLS were lowly expressed in tumor samples ($p < 0.001$). In addition, to further understand the intrinsic association between the ten cuprotosis-related genes, we also performed a correlation analysis. The results showed the most significant positive and negative correlations (Fig. 1B). The above results suggest some interaction between cuprotosis-related genes in gliomas. Then, 365 cuprotosis-related lncRNAs(Table 1) were screened ($|R^2|>0.4$, $p < 0.001$).

Identification of Prognostic Cuprotosis-related lncRNAs and Construction of RS Formula

Univariate Cox regression analysis showed that 295 lncRNAs were associated with patient prognosis. Eighty were considered risk lncRNAs with HR > 1, and 215 were protective lncRNAs with HR < 1. Finally, 12 lncRNAs with the best prognostic relevance were identified after Lasso and multivariate Cox regression (Fig. 1C, D; Table 2). The expression levels of 12 prognostic cuprotosis-related lncRNAs in glioma and normal brain tissue are shown (Fig. 1E). We further visualized the lncRNAs using Cytoscape and “galluvial” R packages. The co-expression network contained 12 lncRNA-mRNA pairs (Fig. 1F). FDX1 was co-expressed with six related genes (AC104117.3, TMEM220-AS1, AL355974.2, LINC01503, CRNDE, and LINC02328) and LIAS with four related genes (AL391834.1, AC084824.4, AC104117.3, AC121761.2, AL391834.1, DNAJC9-AS1, and AC084824.4), GLS co-expressed with SNAI3-AS1 and MTF1 co-expressed with RNF219-AS1. Figure 1G showed that AC084824.4, AC104117.3, AC121761.2, AL391834.1, DNAJC9 - AS1, LINC01503, RNF219-AS1, SNAI3-AS1 were protective factors, while AL355974.2, CRNDE, LINC02328, TMEM220-AS1 were risk factors. We calculated the risk score for each patient in the TCGA dataset using the RS formula. By median risk score, patients were divided into two groups: the high-risk and low-risk groups (Fig. 2A). We found that more and more patients died as the risk score increased (Fig. 2B). Figure 3C shows the 12 prognostic cuprotosis-related lncRNAs involved in both groups by heat map. The ROC curve region shows the good predictive ability of the model based on 12 survival-related lncRNAs. In the TCGA data, the AUC values were 0.896, 0.93, and 0.901 at 1, 3, and 5 years, respectively (Fig. 2D). According to KM analysis, patients with high RS had worse survival than those with low RS (Fig. 2E).

Internal and External Validation of Prognostic Features

Using the same cut-off for the CGGA validation data as for the TCGA data, it was possible to distinguish the high-risk group from the low-risk group. However, the number of patients in the low-risk group was significantly lower (Fig. 2F). CGGA patients showed that high-risk patients were positively associated with poor prognosis (Fig. 2G). The expression of prognostic cuprotosis-related lncRNAs in CGGA was similar to that in TCGA samples (Fig. 2H). In CGGA samples, the AUC values were 0.754, 0.809, and 0.822 at 1, 3, and 5 years, respectively (Fig. 2I). KM analysis performed on the CGGA data showed the same results as the TCGA data ($P < 0.001$, Fig. 2J). The similar validation results presented in the two validation datasets

of TCGA (the AUC values were 0.921, 0.961, and 0.927 at 1, 3, and 5 years; the AUC values were 0.867, 0.893, and 0.71 at 1, 3, and 5 years) also demonstrated the excellent predictive ability of the model (Figure S 1).

To further explore the relationship between risk scores and clinical characteristics of patients, we performed subgroup analysis. We found that risk scores predicted prognosis in different patients (Fig. 3). These results also strengthen the predictive potential of the risk score.

We also evaluated the expression levels of cuprotosis-related lncRNAs in the TCGA dataset. We found that all genes showed significant differences in different classes, and in the validation data CGGA data, all genes except one showed similar trends in other classes (Fig. 4A, B). In both TCGA and CGGA datasets, the expression of genes showed the same trend as the tumor grade increased. PCA analysis showed that high-risk and low-risk patients could be distributed in different quadrants according to RS of prognostic cuprotosis-Related lncRNAs (Fig. 4C-E).

Construction and Validated the Nomogram

We constructed a nomogram based on age, gender, grade, and risk score from TCGA data to facilitate clinical work. First, univariate and multivariate Cox regression analyses showed that age class and risk score were independent predictors of OS in patients with glioma (Fig. 5A, B). Nomograms allow precise calculation of survival probabilities based on patient grade, gender, age, and risk score (Fig. 5C). The calibration curves showed good agreement between actual OS and predicted survival rates (Fig. 5I-K). The ROC curves also validated that the risk score based on cuprotosis-related lncRNAs had the highest predictive accuracy (Fig. 5G). The reliability of the risk score was also validated by analysis of the CGGA data (Fig. 5H, L-N).

Functional Annotation of Cuprotosis-related lncRNAs

We used GSEA to further investigate the biological functions of prognostic features. In the KEGG analysis, the main added features were pathogenic-escherichia-coli-infection, systemic-lupus-erythematosus, cell-cycle, n-glycan-biosynthesis, amino-sugar- and-nucleotide-sugar-metabolism; the reduced functions are taste-transduction, long-term-depression, long-term-potentiation, etc. (Fig. 6A). We quantified the enrichment scores of ssGSEA by measuring immune cell subpopulations and related pathways to investigate further the correlation between risk scores and immune cells and functions. We found that most cells (B cells, CD8 + T cells, DCs, Tregs, etc.) were significantly elevated in the high-risk group (Fig. 6B). T-cell co-stimulation, APC co-stimulation, CCR, T-cell co-stimulation, and type I IFN response were higher in the high-risk group than in the low-risk group (Fig. 6C). The above results suggest that immune function is more active in the high-risk group. Due to the importance of checkpoint-based immunotherapy, we also compared and analyzed the differences in immune checkpoint expression between the two groups (Fig. 6D).

We also analyzed the correlation between predictive characteristics and tumor immune-related drugs. The results found lower IC50 of Cisplatin, Etoposide, and Rapamycin in the high-risk group and higher IC50 of

Lenalidomide and PAC-1 in the high-risk group. (Fig. 6E-I), which helps to explore individualized treatment regimens suitable for the high-risk patient.

Discussion

Glioma is a common intracranial tumor, and the factors that contribute to its development and progression are not fully understood. In-depth studies at the molecular level will help to elucidate the pathogenesis of glioma and predict the prognosis of patients. Cuprotosis is associated with genetic disorders and tumors and has the potential to be a therapeutic strategy(3, 16–18). Recently, several studies have shown that lncRNAs are involved in the development of multiple cancers and that different types of lncRNAs predictive features are used to predict the prognosis of cancer patients (19–21). However, the role of cuprotosis-related lncRNAs in glioma patients has not been reported. Our study identified multiple prognostic cuprotosis-related lncRNAs for the first time and successfully constructed a formula for cuprotosis-related lncRNAs with powerful predictive features, and introduced the role of cuprotosis-related lncRNAs in predicting glioma prognosis and immune status.

This study first extracted ten genes involved in cuprotosis closely and then identified 12 prognostic cuprotosis-related lncRNAs for prognostic signatures using reliable biological analysis. After analysis, AC084824.4, AC104117.3, AC121761.2, AL391834.1, DNAJC9-AS1, LINC01503, RNF219-AS1, SNAI3-AS1 were regarded as protective factors; AL355974.2, CRNDE, LINC02328, TMEM220-AS1 were regarded as risk factors. And among these lncRNAs, the biological functions of some lncRNAs with were confirmed. For example, high expression of CRNDE promotes the malignant progression of gliomas (22). LINC01503 plays an essential role in HCC through the MAPK/ERK pathway(23). TMEM220-AS1 regulates hepatocellular carcinoma by regulating the miR-484/MAGI1 axis(24). Then, we constructed an RS model containing these 12 lncRNAs. Based on the RS model, we divided glioma patients into low-risk and high-risk groups; patients in the high-risk group were shown to have a significantly worse prognosis in both TCGA and CGGA data. To evaluate the reliability of the prognostic features, on the one hand, the risk-risk model was validated by the Kaplan-Meier curve and ROC curve; the correlation analysis of clinical variables and risk scores also increased the reliability of the model.On the other hand, the one-three-and five-year nomograms reported that the model was a good predictor of OS prognosis in glioma patients. The calibration curves further confirmed that the model was accurate. We also analyzed the expression levels of 12 lncRNAs using the TCGA and CGGA databases to verify the reliability of the prognostic features. All genes showed similar trends except for AC084824.4 in the CGGA data. Most importantly, the expression levels of genes that are risk factors increased with increasing tumor grade, while the expression levels of protective genes were reversed.

GSEA shows systemic-lupus-erythematosus, cell-cycle, n-glycan-biosynthesis, amino-sugar-and-nucleotide-sugar-metabolism, leukocyte-transendothelial-migration ware mainly enriched in at-risk groups. It is well known that intracellular metabolic processes such as nucleotides, amino acids, and glutathione play an irreplaceable role in cancer. For example, aberrant glycosylation of cells leads to abnormal expression of membrane-localized glycans, triggering a malignant transformation of cells(25).

N-glycans play an essential role in breast and oral cancers(26, 27). Glutathione affects tumor development by altering the sensitivity to oxidative stress in astrocytic tumors(28). The ssGSEA results showed a significant increase in most cells (macrophages, $CD8^+$ T cells, Neutrophils, mast cells, Tregs, etc.) in the high-risk group. Some studies found that the degree of tumor immune cell infiltration correlated with the prognosis of tumor patients. For example, $CD8^+$ T-cell infiltration was associated with a poor prognosis in BC patients (29). High infiltration of tumor-associated macrophages is associated with poor prognosis in glioma and thyroid cancer(30, 31). The degree of MC infiltration in mouse and human gliomas is proportional to the malignancy of the tumor(32, 33). A high ratio of neutrophils to lymphocytes predicts a poorer OS in BC patients(34). Pathological grading of gliomas is positively correlated with infiltrating neutrophils(35). lncRNA HOXA-AS2 promotes Tregs proliferation and immune tolerance via miR-302a/KDM2A axis, thus promoting glioma progression and poor prognosis (36). An increase in Treg and MDSC in mouse gliomas leads to decreased overall survival (37).In addition to increased tumor immune cell infiltration, immune-related pathways were significantly higher in the high-risk group. In other words, although the immune function was more active in the high-risk group, the decreased anti-tumor immunity of patients in the high-risk group may have contributed to their poor prognosis. This also suggests a new idea for immunotherapy of glioma. Glioma immunotherapy has been a hot topic in recent years (38). Therefore, we also performed an analysis of immune checkpoint expression between high-risk and low-risk groups, hoping to provide some direction for glioma immunotherapy. We studied the sensitivity of immune-related drugs among patients and found that high-risk patients may be sensitive to Cisplatin, Etoposide, Rapamycin, and resistant to Lenalidomide, PAC-1. This implies that high-risk groups may benefit from treatment with multiple immune-related drugs. We hope that the above study provides a basis for precise, individualized treatment of glioma patients.

Although the RS model we constructed has a strong predictive effect. However, there are still some limitations. First, more data are needed to validate the model and improve it. Second, cuprotosis is a newly discovered mode of cell death, and studies about its associated lncRNAs are limited; more studies are needed to elucidate the specific mechanism of how our discovered cuprotosis-related lncRNAs induce cuprotosis.

Conclusion

In conclusion, we screened the lncRNAs with a predictive role in cuprotosis and successfully constructed an RS model with a powerful predictive function. More importantly, this predictive model on cuprotosis provides new ideas for the therapeutic approach to glioma and offers new directions for studying cuprotosis-related lncRNAs in more fields.

Declarations

Data Availability Statement

Publicly available datasets were analyzed in this study. The names of the repository/repositories and accession number(s) can be found in the article

Author Contributions

Shuaishuai Wu had the initial idea for this study, performed the statistical analysis, and wrote the manuscript; Augustine K. Ballah and Wen Qiang Che and Xiang Yu Wang revised the manuscript. All authors contributed to the article and approved the submitted version.

Funding:

No Funding

Conflict of Interests

The authors declare there are no competing interests

Acknowledgments

The authors would like to thank the TCGA, GTEx, CGGA databases, and GSEA websites for data availability.

References

1. Davis ME. Epidemiology and Overview of Gliomas. Semin Oncol Nurs. 2018;34(5):420-9.
2. Bielecka J, Markiewicz-Żukowska R. The Influence of Nutritional and Lifestyle Factors on Glioma Incidence. Nutrients. 2020;12(6).
3. Tsvetkov P, Coy S, Petrova B, Dreishpoon M, Verma A, Abdusamad M, et al. Copper induces cell death by targeting lipoylated TCA cycle proteins. Science. 2022;375(6586):1254-61.
4. Kahlson MA, Dixon SJ. Copper-induced cell death. Science. 2022;375(6586):1231-2.
5. Zhang Z, Ma Y, Guo X, Du Y, Zhu Q, Wang X, et al. FDX1 can Impact the Prognosis and Mediate the Metabolism of Lung Adenocarcinoma. Front Pharmacol. 2021;12:749134.
6. Shin D, Lee J, You JH, Kim D, Roh JL. Dihydrolipoamide dehydrogenase regulates cystine deprivation-induced ferroptosis in head and neck cancer. Redox Biol. 2020;30:101418.
7. Sun J, Li J, Guo Z, Sun L, Juan C, Zhou Y, et al. Overexpression of Pyruvate Dehydrogenase E1α Subunit Inhibits Warburg Effect and Induces Cell Apoptosis Through Mitochondria-Mediated Pathway in Hepatocellular Carcinoma. Oncol Res. 2019;27(4):407-14.
8. Ren X, Li Y, Zhou Y, Hu W, Yang C, Jing Q, et al. Overcoming the compensatory elevation of NRF2 renders hepatocellular carcinoma cells more vulnerable to disulfiram/copper-induced ferroptosis. Redox Biol. 2021;46:102122.

9. Ceyhan D, Guzel KGU, Cig B. The protective role of selenium against dental amalgam-induced intracellular oxidative toxicity through the TRPV1 channel in DBTRG glioblastoma cells. J Appl Oral Sci. 2021;29:e20200414.
10. Illán-Cabeza NA, Jiménez-Pulido SB, Hueso-Ureña F, Ramírez-Expósito MJ, Martínez-Martos JM, Moreno-Carretero MN. Relationship between the antiproliferative properties of Cu(II) complexes with the Schiff base derived from pyridine-2-carboxaldehyde and 5,6-diamino-1,3-dimethyluracil and the redox status mediated by antioxidant defense systems on glioma tumoral cells. J Inorg Biochem. 2020;207:111053.
11. Li Z, Li M, Xia P, Wang L, Lu Z. Targeting long non-coding RNA PVT1/TGF-β/Smad by p53 prevents glioma progression. Cancer Biol Ther. 2022;23(1):225-33.
12. Wang W, Han S, Gao W, Feng Y, Li K, Wu D. Long Noncoding RNA KCNQ1OT1 Confers Gliomas Resistance to Temozolomide and Enhances Cell Growth by Retrieving PIM1 From miR-761. Cell Mol Neurobiol. 2022;42(3):695-708.
13. Gao Y, Yu H, Liu Y, Liu X, Zheng J, Ma J, et al. Long Non-Coding RNA HOXA-AS2 Regulates Malignant Glioma Behaviors and Vasculogenic Mimicry Formation via the MiR-373/EGFR Axis. Cell Physiol Biochem. 2018;45(1):131-47.
14. Rooney MS, Shukla SA, Wu CJ, Getz G, Hacohen N. Molecular and genetic properties of tumors associated with local immune cytolytic activity. Cell. 2015;160(1-2):48-61.
15. Yao J, Chen X, Liu X, Li R, Zhou X, Qu Y. Characterization of a ferroptosis and iron-metabolism related lncRNA signature in lung adenocarcinoma. Cancer Cell Int. 2021;21(1):340.
16. Cui L, Gouw AM, LaGory EL, Guo S, Attarwala N, Tang Y, et al. Mitochondrial copper depletion suppresses triple-negative breast cancer in mice. Nat Biotechnol. 2021;39(3):357-67.
17. Tsang T, Posimo JM, Gudiel AA, Cicchini M, Feldser DM, Brady DC. Copper is an essential regulator of the autophagic kinases ULK1/2 to drive lung adenocarcinoma. Nat Cell Biol. 2020;22(4):412-24.
18. Davis CI, Gu X, Kiefer RM, Ralle M, Gade TP, Brady DC. Altered copper homeostasis underlies sensitivity of hepatocellular carcinoma to copper chelation. Metallomics. 2020;12(12):1995-2008.
19. Gao X, Tang M, Tian S, Li J, Liu W. A ferroptosis-related gene signature predicts overall survival in patients with lung adenocarcinoma. Future Oncol. 2021;17(12):1533-44.
20. Luo H, Ma C. A Novel Ferroptosis-Associated Gene Signature to Predict Prognosis in Patients with Uveal Melanoma. Diagnostics (Basel). 2021;11(2).
21. Zhu L, Yang F, Wang L, Dong L, Huang Z, Wang G, et al. Identification of the ferroptosis-related gene signature in patients with esophageal adenocarcinoma. Cancer Cell Int. 2021;21(1):124.
22. Li DX, Fei XR, Dong YF, Cheng CD, Yang Y, Deng XF, et al. The long non-coding RNA CRNDE acts as a ceRNA and promotes glioma malignancy by preventing miR-136-5p-mediated downregulation of Bcl-2 and Wnt2. Oncotarget. 2017;8(50):88163-78.
23. Wang MR, Fang D, Di MP, Guan JL, Wang G, Liu L, et al. Long non-coding RNA LINC01503 promotes the progression of hepatocellular carcinoma via activating MAPK/ERK pathway. Int J Med Sci. 2020;17(9):1224-34.

24. Cao C, Li J, Li G, Hu G, Deng Z, Huang B, et al. Long Non-coding RNA TMEM220-AS1 Suppressed Hepatocellular Carcinoma by Regulating the miR-484/MAGI1 Axis as a Competing Endogenous RNA. Front Cell Dev Biol. 2021;9:681529.
25. Thomas D, Rathinavel AK, Radhakrishnan P. Altered glycosylation in cancer: A promising target for biomarkers and therapeutics. Biochim Biophys Acta Rev Cancer. 2021;1875(1):188464.
26. Hirano K, Furukawa K. Biosynthesis and Biological Significances of LacdiNAc Group on N- and O-Glycans in Human Cancer Cells. Biomolecules. 2022;12(2).
27. Wu Y, Liu Y, Shang Z, Liu X, Xu Y, Liu W. N-Glycomic profiling reveals dysregulated glycans related to oral cancer using MALDI-MS. Anal Bioanal Chem. 2022;414(5):1881-90.
28. Moreira Franco YE, Alves MJ, Uno M, Moretti IF, Trombetta-Lima M, de Siqueira Santos S, et al. Glutaminolysis dynamics during astrocytoma progression correlates with tumor aggressiveness. Cancer Metab. 2021;9(1):18.
29. Liu Z, Zhou Q, Wang Z, Zhang H, Zeng H, Huang Q, et al. Intratumoral TIGIT(+) CD8(+) T-cell infiltration determines poor prognosis and immune evasion in patients with muscle-invasive bladder cancer. J Immunother Cancer. 2020;8(2).
30. Li G, Li L, Li Y, Qian Z, Wu F, He Y, et al. An MRI radiomics approach to predict survival and tumor-infiltrating macrophages in gliomas. Brain. 2022.
31. Ryder M, Ghossein RA, Ricarte-Filho JC, Knauf JA, Fagin JA. Increased density of tumor-associated macrophages is associated with decreased survival in advanced thyroid cancer. Endocr Relat Cancer. 2008;15(4):1069-74.
32. Põlajeva J, Sjösten AM, Lager N, Kastemar M, Waern I, Alafuzoff I et al. Mast cell accumulation in glioblastoma with a potential role for stem cell factor and chemokine CXCL12. PLoS One. 2011;6(9):e25222.
33. Põlajeva J, Bergström T, Edqvist PH, Lundequist A, Sjösten A, Nilsson G, et al. Glioma-derived macrophage migration inhibitory factor (MIF) promotes mast cell recruitment in a STAT5-dependent manner. Mol Oncol. 2014;8(1):50-8.
34. Tan YG, Eu EWC, Huang HH, Lau WKO. High neutrophil-to-lymphocyte ratio predicts worse overall survival in patients with advanced/metastatic urothelial bladder cancer. Int J Urol. 2018;25(3):232-8.
35. Khan S, Mittal S, McGee K, Alfaro-Munoz KD, Majd N, Balasubramaniyan V, et al. Role of Neutrophils and Myeloid-Derived Suppressor Cells in Glioma Progression and Treatment Resistance. Int J Mol Sci. 2020;21(6).
36. Zhong C, Tao B, Li X, Xiang W, Peng L, Peng T, et al. HOXA-AS2 contributes to regulatory T cell proliferation and immune tolerance in glioma through the miR-302a/KDM2A/JAG1 axis. Cell Death Dis. 2022;13(2):160.
37. Zhai L, Bell A, Ladomersky E, Lauing KL, Bollu L, Nguyen B, et al. Tumor Cell IDO Enhances Immune Suppression and Decreases Survival Independent of Tryptophan Metabolism in Glioblastoma. Clin Cancer Res. 2021;27(23):6514-28.

38. Xu S, Tang L, Li X, Fan F, Liu Z. Immunotherapy for glioma: Current management and future application. Cancer Lett. 2020;476:1-12.

Tables

Tables 1 and 2 are available in the Supplementary Files section

Figures

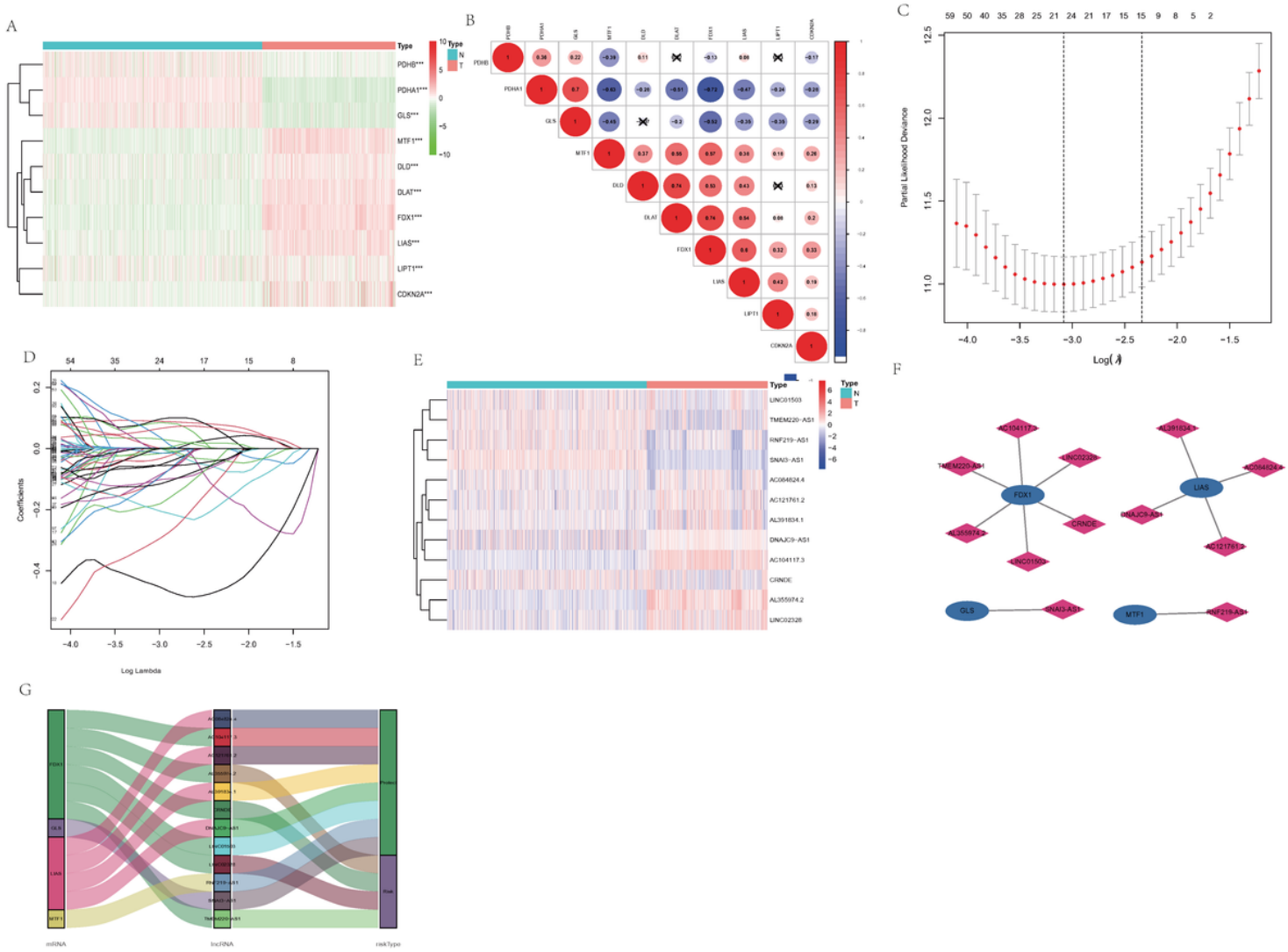

Figure 1

Identification of cuprotosis-related genes and lncRNAs.

(A)The expression levels of cuprotosis-related mRNAs. (B) Spearman correlation analysis of cuprotosis - related mRNAs in glioma. (C)Cross-validation for tuning the parameter selection in the LASSO regression.

(D) LASSO regression of prognosis-related genes. (E)The expression levels of prognostic cuprotosis -Related lncRNAs. (F) The co-expression network of prognostic cuprotosis -related lncRNAs. (G) Sankey diagram of prognostic cuprotosis -Related lncRNAs.

lncRNAs, long noncoding RNAs; N, normal; T, tumor.

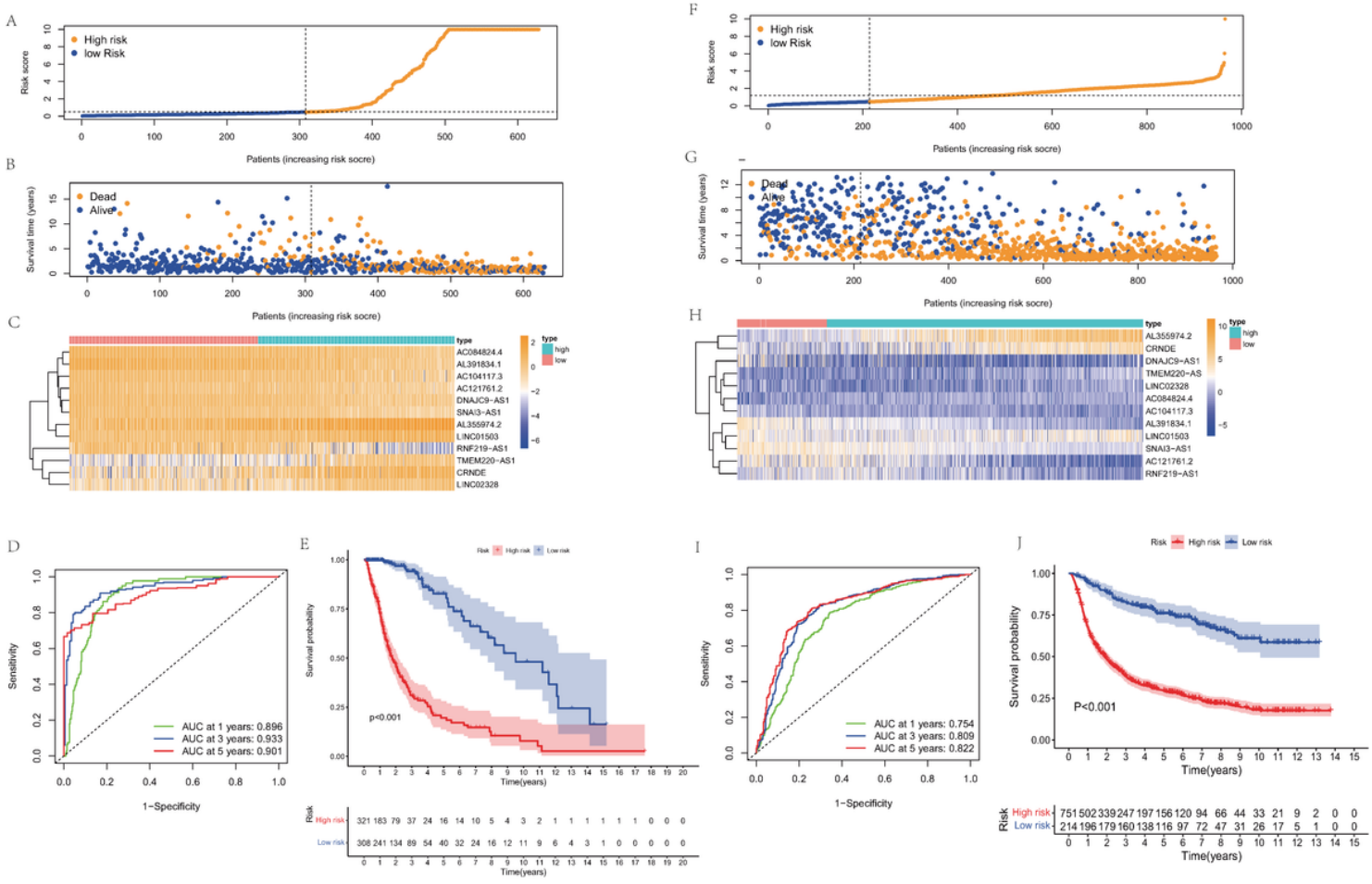

Figure 2

Construction and validation of the prognostic cuprotosis-related lncRNAs signature for survival prediction. (A-E) Distribution of RS; survival time and statu of patients; heatmap of cuprotosis -related lncRNAs of RS; ROC curve; KM curve for TCGA. (F-J) Distribution of RS; survival time and statu of patients; heatmap of cuprotosis -related lncRNAs of RS; ROC curve; KM curve for CGGA.

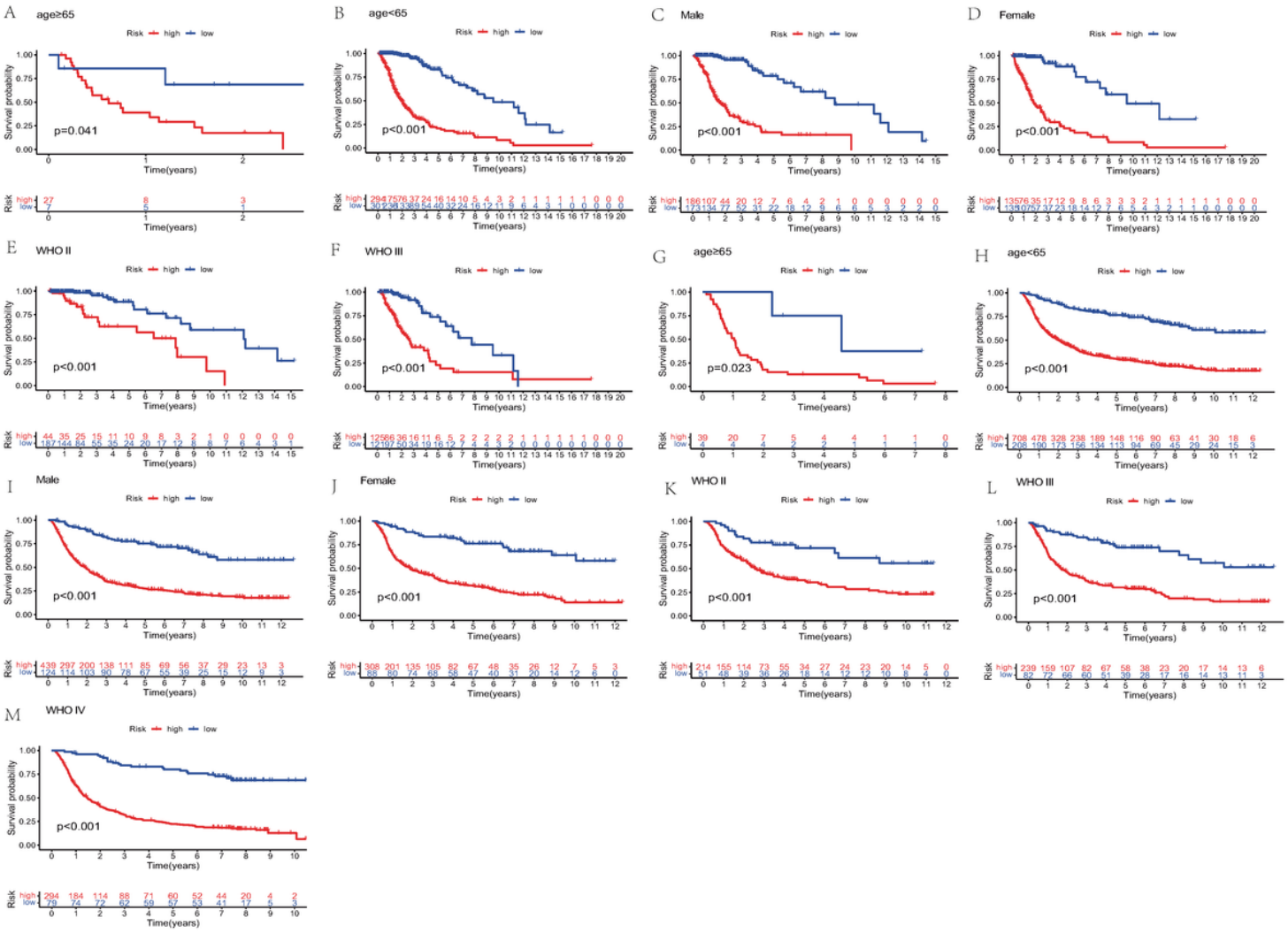

Figure 3

Subgroup analysis of high- and low-risk group. (A-F) Subgroup analysis s of TCGA data. (G-M) Subgroup analysis s of CGGA data.

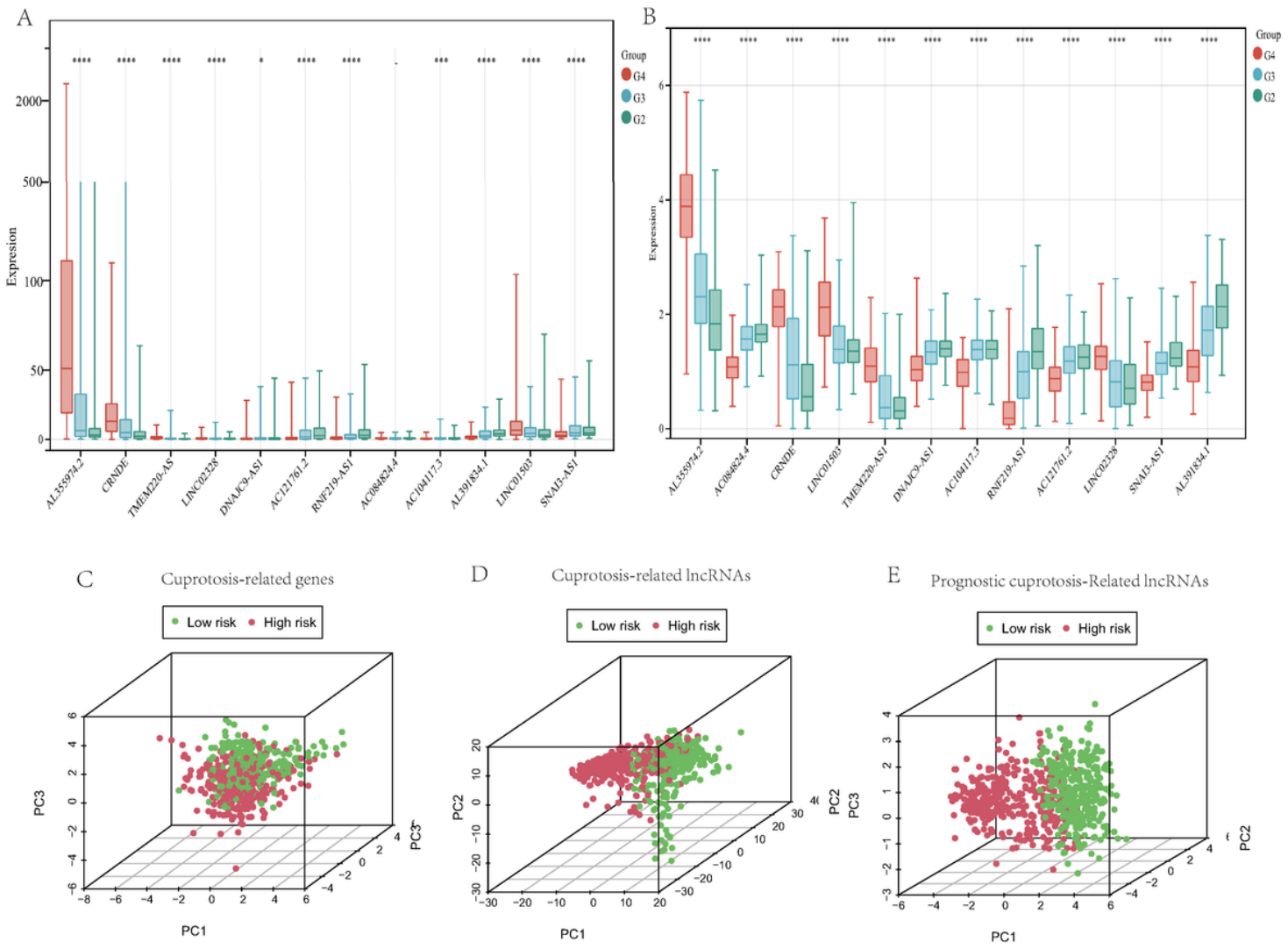

Figure 4

Expression profile of 12 prognostic cuprotosis -related lncRNAs with different glioma grades. (A)m7G-related lncRNAs expression with different glioma grades in CGGA datasets. (B) prognostic m7G-Related lncRNAs expression with different glioma grades in TCGA datasets. (G2: Grade II, G3: Grade III, G4: Grade IV). * P < 0.05, ** P < 0.01 and *** P < 0.001.

PCA analysis of the samples in the TCGA glioma dataset. (C) Cuprotosis-related genes; (D) Cuprotosis-related lncRNAs; and (E) Prognostic cuprotosis-Related lncRNAs

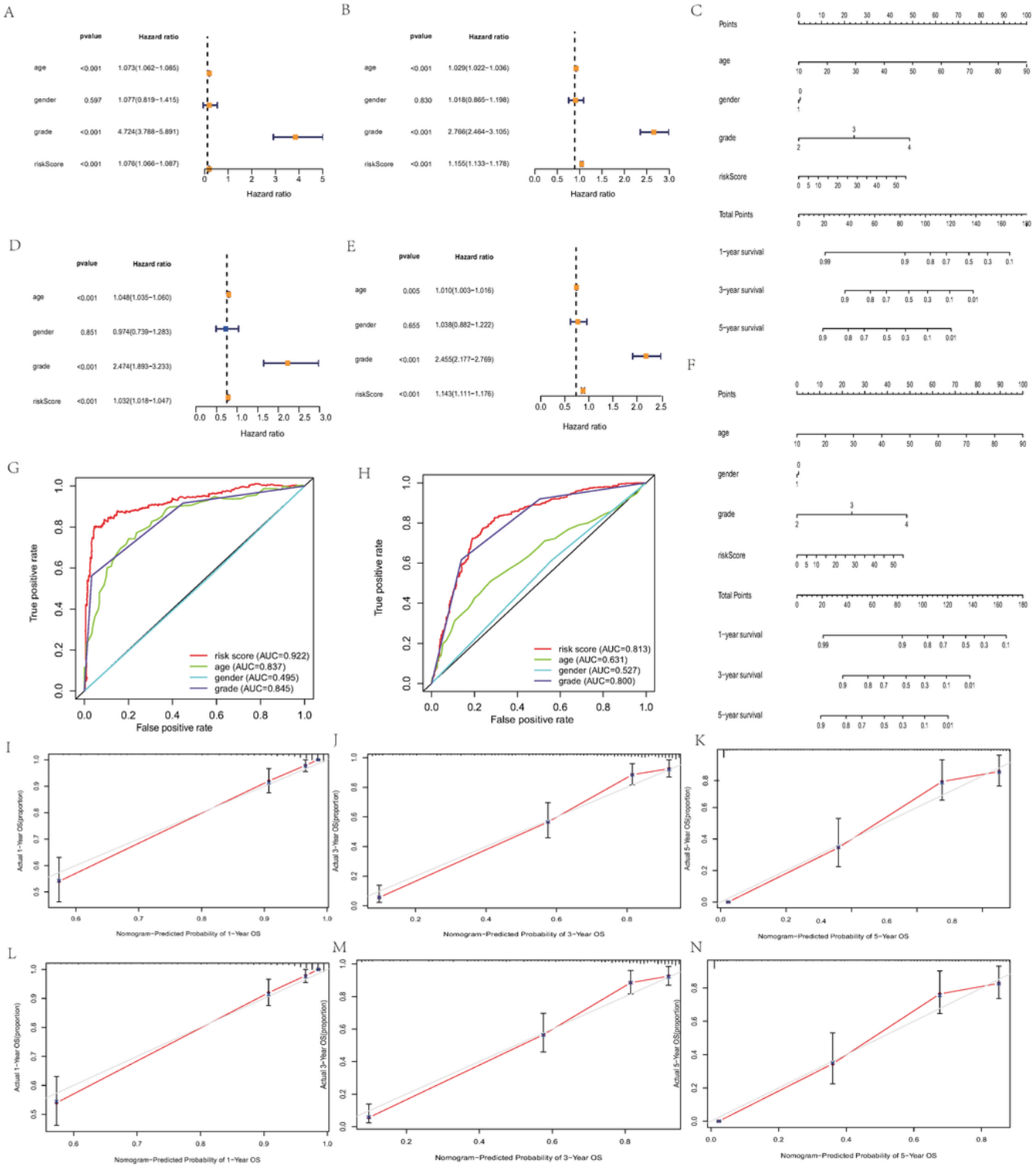

Figure 5

Independent prognosis analysis of risk score. (A, D) Univariate COX Forest plot of risk score in TCGA and in CGGA. (B, E) Multivariate COX Forest plot of risk score in TCGA and CGGA. (C, F) Nomogram based on prognostic features in TCGA and CGGA. (G, H) ROC curves for the nomogram, risk score, age and grade in TCGA and CGGA. (I-K) Calibration plots of the nomogram for predicting the probability of OS at 1, 3, and

5 years in the TCGA. (L-N) Calibration plots of the nomogram for predicting the probability of OS at 1, 3, and 5 years in the CGGA.

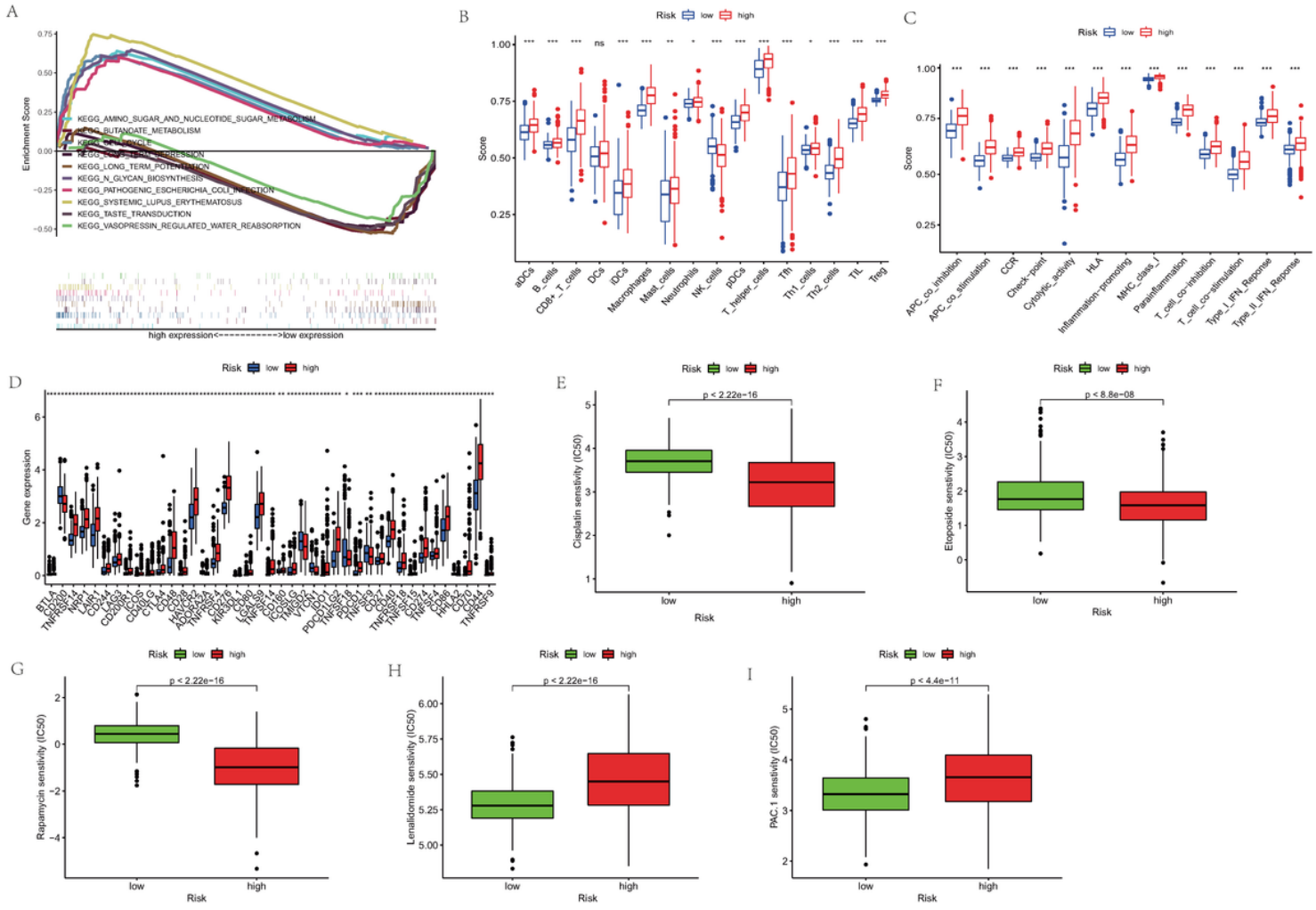

Figure 6

Functional enrichment analysis of 8 prognostic m7G-Related lncRNAs. (A)KEGG analysis of 8 prognostic m7G-Related lncRNAs. (B) The infiltration levels of 16 immune cells. (C) The correlation between the predictive signature and 13 immune-related functions. (D) Expression of immune checkpoints.

aDCs, activated dendritic cells; iDCs, immature dendritic cells; NK, natural killer; pDCs, plasmacytoid dendritic cells; Tfh, T follicular helper; Th1, T helper type 1; Th2, T helper type 2; TIL, tumor-infiltrating lymphocyte; Treg, T regulatory cell; APC, antigen-presenting cell; CCR, chemokine receptor; HLA, human leukocyte antigen; MHC, major histocompatibility complex; IFN, interferon. *p < 0.05; **p < 0.01; ***p < 0.001; ns, non-significant.

Comparison of treatment drugs senstivity between high- and low-risk groups. (E-I) IC50 of Cisplatin, Etoposide, Rapamycin, Lenalidomide, PAC.1 in high and low risk groups. IC50, half-maximal inhibitory concentration.

Supplementary Files

This is a list of supplementary files associated with this preprint. Click to download.

- Table2PrognosticCuprotosisrelatedlncRNAs.xls
- Table1CuprotosisrelatedlncRNAs.xlsx
- figureS1.pdf